10th International Conference on Fracture Mechanics of Concrete and Concrete Structures
FraMCoS-X
G. Pijaudier-Cabot, P. Grassland C. La Borderie(Eds)
https://doi.org/10.21012/FC10.235643

EVALUATION OF RESIDUAL ELASTICITY OF AN INTERNAL EXPANSION-INDUCED CONCRETE

F. CHEN*, J. SANAHUJA†, B. BARY††, AND Y. LE PAPE†††

*Den-Service d'Etude du Comportement des Radionucléides (SECR), CEA,
Université Paris-Saclay, F-91191, Gif-sur-Yvette, France.
E-mail: fengjuan.chen@cea.fr

†Materials Ageing Institute (MAI), EDF R&D/MMC, Site des Renardières
Ecuelles, F-77250, Moret-sur-loing, France.
E-mail: julien.sanahuja@edf.fr

††Den-Service d'Etude du Comportement des Radionucléides (SECR), CEA,
Université Paris-Saclay, F-91191, Gif-sur-Yvette, France.
E-mail: benoit.bary@cea.fr

†††Oak Ridge National Laboratory (ORNL), Oak Ridge, TN 37831, USA.
E-mail: lepapeym@ornl.gov

Keywords: Meso-scale, Microcracking, Residual elasticity, Internal expansion, Brittle material.

Abstract: This paper addresses the degradation due to neutron radiation exposures of concrete consisting in various rock-forming silicate-based aggregates and cement paste. We are interested in the evaluation of the residual elastic properties of concretes subjected to a high fluence of fast neutron irradiation by means of an extended composite sphere model. We first introduce briefly the main features of the model, and then show how the damage resulting from the aggregate expansion generated by their physical and structural changes upon irradiation can be captured and accounted for. To validate the established analytical solutions of the model and illustrate its predicting performance, we apply it on two specific concretes: (1) a concrete consisting of an ordinary cement paste and silicate-based aggregates of various sizes; and (2) a concrete consisting of massive serpentine aggregates and a pure aluminous cement paste. In both cases, the model predictions are compared with the available experimental measurements, and a good accordance between them is found. The composite sphere model gives a full description of the damage development in the mortar and identifies the primary role of the aggregate expansion on the material degradation mechanisms. In this first attempt, only damage in the mortar is accounted for in the modelling while the aggregates are assumed to behave elastically.

1 INTRODUCTION

In nuclear power stations, the concrete biological shield wall surrounding reactor containing vessel is exposed to different ionizing irradiation effects including neutrons and gamma-ray. In addition, irradiation-induced energy-deposition causes internal heating and radiolysis. According to [1], " A recent report of the U.S. Nuclear Regulatory Commission / Department of energy has identified irradiation effects and alkali-silica reaction [ASR:…] as key degradation mechanisms that require priority research in

the context of license renewal and LTO of the U.S. commercial nuclear fleet. In spite of several past and ongoing studies, comprehension of the effects of irradiation on the mechanical and physical properties of concrete remains very limited." In the current paper, we focus on the effects of fast-neutron irradiation-induced volumetric expansion of the aggregates as the main degradation mechanism of concrete.

To accurately describe the damage evolution in the concrete and the resulting residual elasticity, we propose an extended composite sphere model on the basis of [2] and perform a first validation of the established solutions by comparing the model predictions with experimental data available in the open literature on two specific concretes.

2 GENERAL FEATURES

In the thermodynamic framework of the continuum damage mechanics (CDM), we consider an elastic material with isotropic damage represented by randomly orientated similar penny-shaped microcracks. The anisotropy induced by the damage is out of the scope of the current paper. At a given damage level, the considered material is assumed to be linear elastic, the dissipated energy per unit volume at the macroscopic scale is defined as the difference between the mechanical work and the increment of the energy stored in the solid (see [2][3]):

$$D = \boldsymbol{\sigma}:\dot{\boldsymbol{\varepsilon}} - \dot{\Psi} = -\frac{\partial \Psi}{\partial d}\dot{d} \qquad (1)$$

Here, d denotes the crack density parameter and the free energy Ψ reads as $\Psi = \frac{1}{2}\boldsymbol{\varepsilon}:\mathbf{C}(\mathbf{d}):\boldsymbol{\varepsilon}$. In general, the term $-\partial\Psi/\partial d$ is referred to as the driving force $F(d)$ of the damage process, and $F(d)$ can be expressed in terms of the compliance (resp. stiffness) tensor of the damaged solid:

$$F(d) = -\frac{1}{2}\boldsymbol{\varepsilon}:\frac{\partial \mathbf{C}(\mathrm{d})}{\partial \mathrm{d}}:\boldsymbol{\varepsilon} = \frac{1}{2}\boldsymbol{\sigma}:\frac{\partial \mathbf{S}(\mathrm{d})}{\partial \mathrm{d}}:\boldsymbol{\sigma} \qquad (2)$$

Following the definition of the damage yield function $f(F(d), d) = F(d) - \kappa(d)$ where $\kappa(d)$ represents the resistance of a material to the damage propagation, $F(d)$ can be considered as an indicator of the damage propagation.

An alternative definition of the dissipated energy is expressed as $D = \mathrm{G}_c\dot{d}$ with G_c being referred to as critical energy (see [2]). For being consistent between the two definitions, the following condition needs to be met:

$$\mathrm{G}_c = \frac{1}{2}\boldsymbol{\sigma}:\frac{\partial \mathbf{S}(\mathrm{d})}{\partial \mathrm{d}}:\boldsymbol{\sigma} \text{ If } \dot{d} > 0 \qquad (3)$$

In general, Eq. (3) is referred to as the damage evolution law.

The derivative of $F(d)$ with respect to d is referred to as the damage stability condition, that is:

$$\frac{\partial F(d)}{\partial d} = -\frac{1}{2}\boldsymbol{\varepsilon}:\frac{\partial^2 \mathbf{C}(\mathrm{d})}{\partial \mathrm{d}^2}:\boldsymbol{\varepsilon} = \frac{1}{2}\boldsymbol{\sigma}:\frac{\partial^2 \mathbf{S}(\mathrm{d})}{\partial \mathrm{d}^2}:\boldsymbol{\sigma} \qquad (4)$$

Eq. (2-4) identified the key role of the compliance (resp. stiffness) tensor of the damaged solid in determining the critical energy and the damage stability condition.

By taking the example of the concrete, we discuss the damage evalution in a quasi-brittle material in the current paper. Figure 1 illustrates the multiple length scales of a damaged concrete structure whereas the coarse aggregate, the damaged and undamaged elastic matrix are represented by red spherical solid, dark gray and light gray solid, respectively. It is assumed that the damage is developed extensively in the matrix while the aggregates deform elastically.

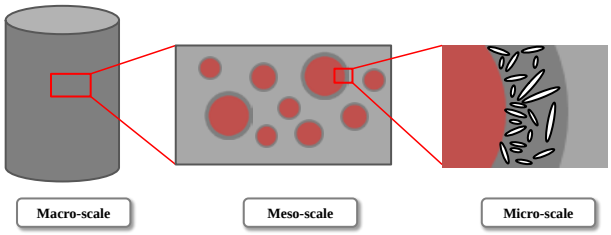

Figure 1: Concrete multiple length scales

At the mesoscopic sale, the concrete can be considered as a 2-phase material including the aggregates and an elastic damageable mortar matrix. Under fast-neutron irradiation, the aggregates are subject to amorphization, i.e., a gradual loss of crystallinity generally

accompanied by significant change of volume (up to 18% in quartz). The radiation-induced volumetric expansion causes the formation of microcracking in the concrete that can affect its physical properties. Figure 2 illustrates the proposed evolution of damage in the matrix surrounding a swelling aggregate:

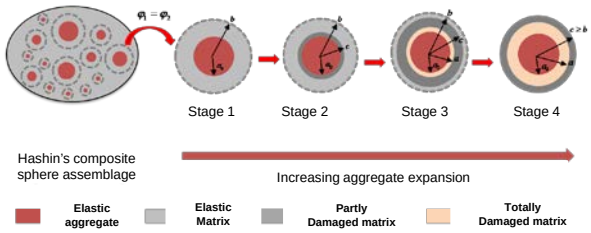

Figure 2: Illustration of the proposed evolution of damage

Stage 1: Before the formation of any initial damage, the composite sphere model consists of a linear elastic aggregate and an elastic damageable mortar matrix. They are represented by a central sphere of radii $r = a_0$ and the volume enclosed between two concentric spheres of radii $r = a_0$ and $r = \mathrm{b}$, respectively.

Stage 2: Once the critical fracture energy G_c of the matrix is reached, damage develops through the formation of microcracks and propagates towards the periphery of concrete. In the initial stage of damage, the adjacent area of the aggregate-matrix interface enclosed between two concentric spheres of radii $r = a_0$ and $r = \mathrm{c}$ loses progressively its stiffness while the microcracks propagate towards $r = c$ ($a_0 < c < b$), and the outer portion remains elastically. Here, c denotes the location of the boundary that delineates the damaged and undamaged matrix. It is worth emphasizing that, at a given value of c, the crack density parameters of microcracks $d(r)$ decreases from the aggregate-matrix interface, and the minimum value of the stiffness is reached at the aggregate-matrix interface. In order to ensure the positive value of the stiffness, c must not exceed a critical value c_r, that is, if $a_0 < c < c_r$, the whole matrix is divided into a damaged and undamaged portion by the boundary $r = c$. We give the analytial solutions of $d(r)$ and c_r in section 2.2.

Stage 3: The local stiffness of the aggregate-matrix interface reaches 0 at $c = c_r$. If the aggregate continue to swell, the value of c exceeds its critical value (that is $c_r < c < b$) , and the volume enclosed between the two concentric spheres of radii $r = a_0$ and $r = \mathrm{a}$ completely loses its stiffness (marked in orange color in figure 2).

Stage 4: If $c_r \geq b$, the volume enclosed between two concentric spheres of radii $r = a_0$ and $r = \mathrm{a}$ completely loses its stiffness and the outer portion of the matrix is damaged.

In the following analysis, we show how to calculate the mechanical fields (stress and strain) resulting from fast-neutron irradiation-induced volumetric expansion of the aggregates by means of the extended composite sphere model.

2.1 Elastic model

The composite sphere model respects a spherical symmetry. As long as the constituents remain governed by isotropic elasticicity, their displacement fields can be sought in the radial form $\underline{U} = U_r \underline{e_r}$ in the spherical coordinate and U_r for the constituents read:

$$Aggregate: U_r = Ar \quad (5)$$

$$Mortar: U_r = Br + C/r^2 \quad (6)$$

The stiffness tensor of each constituent of the concrete can be formulated in the form of $\boldsymbol{C} = 3\mathrm{K}\mathbf{J} + 2\mu\mathbf{K}$ with the fourth-rank tensor being defined as $J_{ijkl} = \frac{\delta_{ij}\,\delta_{kl}}{3}$ and $K_{ijkl} = \frac{(\delta_{il}\delta_{jk} + \delta_{ik}\delta_{jl})}{2}$.

By substitution of $\boldsymbol{C}$ and $\underline{U}$ into the Navier equation $div(\boldsymbol{C}: \nabla \underline{U}) = 0$, we obtain a second-order ordinary differential equation, and the stress components of each constituent of the concrete can be expressed in terms of the displacement field:

Aggregate:

$$\sigma_{rr} = \sigma_{\theta\theta} = \sigma_{\varphi\varphi} = 3k_1(A - \varepsilon_{irr}(n)) \quad (7)$$

Mortar:

$$\sigma_{rr} = 3k_0 B - \frac{4\mu_0 C}{r^3}$$

$$\sigma_{\theta\theta} = \sigma_{\varphi\varphi} = 3k_0 B + \frac{4\mu_0 C}{r^3} \quad (8)$$

$\varepsilon_{irr}(n)$ denotes the fast-neutron irradiation-induced volumetric expansion of the aggregates, and "1" and "0" respectively denote the aggregate and the matrix.

The solutions of the unknown coefficients A, B and C are derived from:

- The absence of external pressure: $\sigma_{rr} = 0$ at $r = b$.
- The continuity of stress and displacement in the radial direction at $r = a_0$.

The macroscopic strain of the concrete in the radial direction $\varepsilon_{rr}^{con} = U(b)/b$ defines the irradiation-induced expansion of concrete over time:

$$\varepsilon_{rr}^{con} = \frac{\varepsilon_{irr}(n)}{3} \frac{k_1 a_0^3 (3k_0 + 4\mu_0)}{4\mu_0 a_0^3 (k_1 - k_0) + k_0 b^3 (3k_1 + 4\mu_0)} \quad (9)$$

2.2 Damage model

Once the critical fracture energy G_c is reached, microcracking develops in the matrix. For the sake of simplicity and following [2], we assume microcracks remain closed, which, in consequence, affects greatly the shear modulus of the matrix, but not its bulk modulus. The latter can be estimated by various homogenization schemes in the context of micromechanical theory of microcracked materials. We adopted the classical Pont Castañeda–Willis (PCW) model (see [4]):

$$\mu(d) = \mu_0 \frac{1+Qd}{1+Q'd} \quad (10)$$

with

$$Q = \frac{32(5\vartheta_0 - 7)}{225(2-\vartheta_0)}, \; Q' = \frac{64(4-5\vartheta_0)}{252(2-\vartheta_0)} \quad (11)$$

ϑ_0 denotes the Poisson's ratio of the undamaged matrix.

Extending the same reasoning previously developed for the undamaged matrix, the stress components of the damaged matrix are expressed in terms of the radial displacement field:

$$\sigma_{rr} = \left(k_0 - \frac{2}{3}\mu(d)\right)\left(\frac{\partial U}{\partial r} + 2\frac{U}{r}\right) + 2\mu(d)\frac{\partial U}{\partial r}$$

$$\sigma_{\theta\theta} = \sigma_{\phi\phi} = \left(k_0 - \frac{2}{3}\mu(d)\right)\left(\frac{\partial U}{\partial r} + 2\frac{U}{r}\right) + 2\mu(d) \quad (12)$$

and then, G_c can be reformulated as :

$$G_c = -\frac{2}{3}\frac{\partial \mu}{\partial d}\left(\frac{\partial U}{\partial r} - \frac{U}{r}\right)^2 \quad (13)$$

We are left with determining the displacement field of the damaged matrix. By substitution of $\mu(d)$ into eq.(13), we obtain:

$$U_r = u_0 r + r\int_{a_0}^{r} \frac{\xi\left(1 + Q'd(\rho)\right)}{\rho} d\rho$$

$$\text{with } \xi = \pm\sqrt{\frac{3}{2(Q'-Q)\mu_0}}\sqrt{\frac{1}{2}\boldsymbol{\sigma}:\frac{\partial \mathbf{S}(\mathrm{d})}{\partial \mathrm{d}}:\boldsymbol{\sigma}} \quad (14)$$

Combining Eqs. (10-14), we derive the analytical solutions of the stress fields:

$$\sigma_{rr} = 3K_0 u_0 + \frac{12K_0\mu_0\xi(Q-Q')}{(3k_0Q'+4\mu_0Q)}\ln(r) +$$

$$\frac{4}{3}\frac{\mu_0\xi Q(3k_0+4\mu_0)}{(3k_0Q'+4\mu_0Q)}\left(\frac{\mathrm{c}}{\mathrm{r}}\right)^3$$

$$\sigma_{\theta\theta} = \sigma_{\varphi\varphi} = 3k_0 u_0 + \frac{12k_0\mu_0\xi(Q-Q')}{(3k_0Q'+4\mu_0Q)}\ln(r) +$$

$$\frac{2\mu_0\xi}{3(3k_0Q'+4\mu_0Q)}\Big(9k_0(Q-Q') - Q(3k_0 +$$

$$4\mu 0\mathrm{cr}3 \quad (15)$$

u_0 is derived from expressing the continuity of the radial stress at $r = a_0$:

$$u_0 = \frac{4\mu_0\xi(Q'-Q)}{(3k_0Q'+4\mu_0Q)}\ln(a_0) - \frac{k_1}{3(k_0-k_1)}\varepsilon_{irr}(n) -$$

$$\frac{\xi(3k_0+4\mu_0)(3k_1Q'+4\mu_0Q)}{9(k_0-k_1)(3k_0Q'+4\mu_0Q)}\left(\frac{c}{a_0}\right)^3 \quad (16)$$

The irradiation-induced expansion of concrete reads:

$$\varepsilon_{rr}^{con} = \frac{U(b)}{b} = -\frac{1}{9}\frac{c^3\xi(3k_0+4\mu_0)}{k_0 b^3} \quad (17)$$

c depends on the volumetric expansión of the aggregates and their relationship can be derived from the continuity of of stress field in the radial direction at $r = c$.

By substitution of eq. (15-16) into the Navier equation with condition $d(c)$ =0, we obtain the crack density parameter $d(r)$ being expressed in terms of r:

$$d(r) = \frac{3k_0+4\mu_0}{3k_0Q'+4\mu_0Q}\left(\left(\frac{c}{r}\right)^3 - 1\right) \quad (18)$$

and to accurately describe the transition from stage 2 to stage 3, we derive the analytical solution of c_r. As stated before, if c reaches the critical value c_r, the stiffness of the aggregate-matrix interface reaches to 0, thus, we obtain:

$$c_r = a_0\left(\frac{1-Q'/Q}{1+4\mu_0/3k_0}\right)^{1/3} \quad (19)$$

3 EXPERIMENTAL DATA

In this section, we validate the established solutions by comparing the model predictions with experimental data available in the open litterature. To this end, we apply the composite sphere model on two specific concretes .

3.1 A concrete with tuff aggregates containing 92% quartz

A principal data resource is [5], the authors investigated experimentally the influences of various irradiation resources on the dimensional changes, the physical properties alterations and their underlying mechanisms of various specimens involving white cement paste, aggregate, and concrete.

According to [5], “Among the rock-forming minerals, α-quartz is the most sensitive to the neutron irradiation”, the authors performed their experimental tests using various concrete specimens that are denoted by Con-A and Con-B in their work. For instance, Con-A is made up of tuff aggregates, which include 92% quartz, and Con-B contains river gravel, which include half of the quartz than tuff. The tuff aggregate is denoted by GA while the river gravel aggregate is denoted by GB. The authors measured the expansion of aggregates and concrete at various fluences of fast neutron irradiation.

In the current study, we consider a specific concrete containing 92% α-quartz in order to illustrate the effects of aggregate expansion on the concrete expansion. Following [5], we adopted the nucleation and growth model ([6]) to characterize the expansive behavior of the considered aggregates:

$$\varepsilon_{irr}(n) = \varepsilon_{\infty}^{quartz}\left(1 - exp\left(-\left(\frac{n}{K(T)}\right)^{dim}\right)\right) \quad (20)$$

with

$$K(T) = 0.45 \times 10^{20} \times \frac{exp\,(2000/298)}{exp\,(2000/T)} \quad (21)$$

$\varepsilon_{\infty}^{quartz}$ = 17.8% denotes the volumetric expansion of quartz up to a fully amorphized state, $K(T)$ denotes the fast-neutron fluence when the expansion reaches half of the maximum expansion volume and the dimensionless coefficient dim is taken as 2.38. Besides, temperature T is expressed in Kelvin and coefficient 0.45×10^{20} governs the shape of the aggregate expansion curve. The nucleation and growth model depends on the temperature. Figure 3 shows the expansive behavior of GA characterized by the nucleation and growth model at different temperatures.

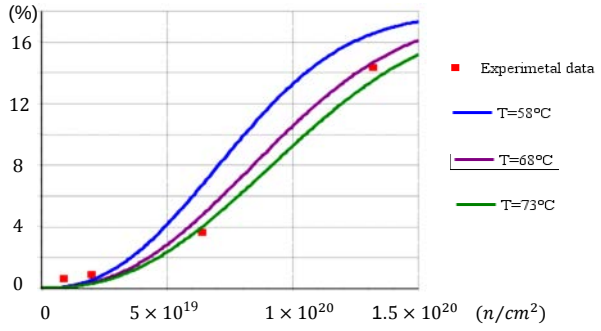

Figure 3: Comparaison between the volumetric expansion of aggregate GA calculated by the nucleation and growth model at different temperatures (continuous curves) and the experimental measurement of the same (red dot) captured from figure 42 of [5].

The static elastic parameters employed in

the composite sphere model are computed from the corresponding dynamic parameters. [5] provided many experimental measurements of the dynamic elastic modulus, we use them directly without modification. For the dynamic elastic modulus that are not provided in [5], we consider their classical values. In the following strucutre, we show how to determine the statistic elastic modulus from the dynamic ones.

Elastic modulus of the aggregate

The dynamic Young's modulus and the Poisson's ratio of GA are measured experimentally and illustrated in figure 100 of [5], $E_1^d = 68Gpa$ and $\vartheta_1^d = 0.28$. For getting the static Young's modulus of the aggregate, we adopt the empirical formula provided in [7]:

$$log_{10}^{E} = 0.02 + 0.77 log_{10}^{(\rho E_d)} \qquad (22)$$

The mass density of aggregate GA is given in Table 9 of [5] , $\rho_1 = 2.66\, g/cm^3$. Thus, eq.(22) gives the static Young's modulus of the aggregate 57.3GPa. As for the static Posson's ratio, no obvious correlation between the dynamic and static Poisson's ratio has been found for the rock-forming aggregate. However, knowing that the dynamic elastic property is in general higher than the static one (see [8][9]), we consider an arbitrary value of $\vartheta_1 = 0.25$ in the current study.

Elastic modulus of the matrix and the volume fraction of aggregate

The authors didn't provide the Young's modulus and Poisson's ratio of the mortar matrix but they measured these parameters for Con-A. The Young's modulus is shown in figure 37(d) of [5], $E_d^{cond} = 38.1GPa$. To get the static elastic modulus of Con-A,we adopt the following formula ([10]):

$$E_{con} = \frac{446.09 E_d^{1.4}}{\rho^c}(GPa) \qquad (23)$$

ρ^c denotes the mass density of Con-A, $\rho_{\text{con}-\text{A}} = 2.34\ \text{g/cm}^3$(see table 10 in [5]). We obtain the static Young's modulus of Con-A, $\text{E}_{\text{con}} = 31.15\ \text{GPa}$. However, the static Poisson's ratio is not provided in [5], but its value ranges in general from 0.20 to 0.30, in the current comparison, we take $\vartheta_{\text{con}} = 0.22$. Conventially, the bulk and shear modulus of Con-A can be calculated using Hook's law for a continuum medium: $\text{K}_{\text{con}} = 18.43\text{GPa}$, $\mu_{\text{con}} = 12.79\text{GPa}$.

For getting the static Young's modulus and the Poisson's ratio of the matrix, we suggest applying inverse analysis, based on the micromechanical model provided in [11]. The effective bulk and shear modulus of a 2-phase material can be calculated by the following equations (refer to eq. 46 and eq. 51 of [11]):

$$K_{con} = K_0 + \frac{\emptyset}{\frac{1}{K_1 - K_0} + 3(1-\emptyset)\frac{1}{3K_1 + 4\mu_1}}$$

$$A_c \left(\frac{\mu_{con}}{\mu_0}\right)^2 + B_c \left(\frac{\mu_{con}}{\mu_0}\right) + C_c = 0 \qquad (24)$$

with coefficients A_c , B_c and C_c being expressed in terms of the radius r, Poisson's ratio of the matrix ν_0 and the aggregate ν_1. Explicite solutions of A_c, B_c and C_c are given in equations (27-29) and (50-51) in [11] ($\text{n} = 2$ and $k = 1$) , and K_{con} and μ_{con} respectively denote the bulk and shear moduli of the concrete and the volume fraction of aggregate $\emptyset = 37.4\%$ can be obtained using the provided data of table 9 and 10 in [5]. Thus, we obtain the static Young's modulus and the Poisson's ratio of the matrix: $E_0 = 22.3Gpa, \vartheta_0 = 0.205$ using eq. (24).

Figure 4 shows the comparison of the concrete volumetric expansion calculated by the composite sphere model and experimental data provided in [5]: damage initializes in the matrix once the fast neutron irradiation fluence reaches $n \approx 3.1 \times 10^{19}\, n/cm^2$ and the matrix loses completely its stiffness at $n \approx 5.3 \times 10^{19}\, n/cm^2$. It is seen that the composite sphere model underestimates the concrete expansion, this may possibly due to the fact thatonly the volumetric expansion of coarse aggregates is accounted for in the currently proposed composite sphere model, the irradiation-induced expansion of aggregates

that disperse in the matrix.

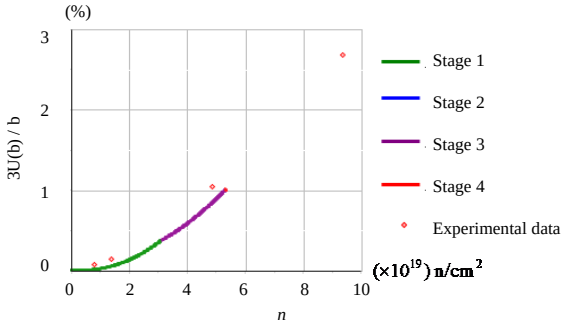

Figure 4: comparison of the concrete volumetric expansion: results calculated by the composite sphere model is illustrated by lines and the experimental measurements of [5] are shown by points for 7.76×10^{18}, 1.41×10^{19},4.52×10^{19} and $9.11 \times 10^{19}\ n/cm^2$ fluences , resp.

3.2 Concrete consisting in massive serpentine aggregates

Further comparison is conducted to assess the validity of the effective properties estimations. As described above, based on the Ponte Castañeda–Willis estimates, the shear modulus $\mu(d)$ depends on the radius r and is then non homogeneous in the damaged region surrounding the aggregates. In order to account for such a heterogeneous region in the calculation of effective properties, we suggest to divide the damaged matrix into N layers of the same width, and N should be large enough so that the effective shear modulus can be considered constant in each layer. In the volume limited by two concentric spheres of radius r_{n-1} and r_n, using the PCW estimation (equation 10-11), the shear modulus μ_n can be calculated by the following equations:

$$\mu_n = \frac{\mu_0(1+Qd_{n-1})}{2(1+Q'd_{n-1})} + \frac{\mu_0(1+Qd_n)}{2(1+Q'd_n)}, n \geq 2 \qquad (25)$$

with $d(r)$ given in eq. (18) :

$$d_{n-1} = \frac{(3k_0+4\mu_0)}{3k_0Q'+4\mu_0Q}\left(\left(\frac{c}{r_{n-1}}\right)^3\right) \qquad (26)$$

and

$$d_n = \frac{(3k_0+4\mu_0)}{3k_0Q'+4\mu_0Q}\left(\left(\frac{c}{r_n}\right)^3\right) \qquad (27)$$

Conventionally, the composite sphere is transformed into a sphere with n layers and each layer is homogeneous and isotropic (illustrated in figure 5). The effective elasticity can be calculated using eq. (24). We clarify that the effective modulus calculated here corresponds to the static quantities, and they need to be converted to the dynamic ones for further comparison with adequate data. For instance, the static Young's modulus can be converted to the dynamic one using eq. (23).

Ultrasonic testing is frequently practiced to assessthe material quality and its physical properties. The ultrasonic pulse velocity V_p is related to the dynamic Young's modulus E_d and dynamic Poisson's ratio ϑ_d of the material by the following equation:

$$V_p = \sqrt{\frac{E_d}{\rho}\frac{1-\vartheta_d}{(1+\vartheta_d)(1-2\vartheta_d)}} \qquad (28)$$

where ρ denotes the mass density. This is the reason why we calculate the dynamic Young's modulus in the previous section. With eq. (28), we obtain the ultrasonic pulse velocity by making use of the composite sphere model and the n-layered inclusion-based micromechanical model ([11]).

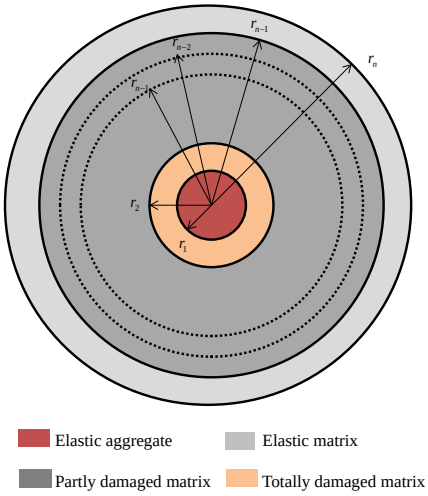

Figure 5: n-layered inclusion-based micromechanical model applied to the damaged zone of the current problem

To verify the established solution of the ultrasonic pulse velocity, the analytical result is compared with experimental measurements on a specific concrete sample. We consider a concrete consisting of massive serpentine

aggregates and a pure aluminous cement paste. The physical properties of aggregate and concrete, which will be used as model inputs in the composite sphere model, can be calculated from the experimental data given in [12]. For instance, the ultrasonic pulse velocity for the concrete and the aggregates are measured as $5260m/s$ and $7140m/s$, the mass densities for the same are measured as $2.51g/cm^3$ and $2.55g/cm^3$ (see Table I and Table II in their paper), respectively. As no information of the Poisson's ratio of the concrete is found in [12], we take a classical value of $\nu_{con} = 0.20$. The volume fractions of aggregates of various sizes are given. In the current context of the composite sphere model, we consider only the coarse aggregates with size varying from 5 to 12 mm. The static Young's modulus and Poisson's ratio of the matrix are not provided in [12], but they can be calculated by the self-consistent effective matrix homogenization (eq. 24).

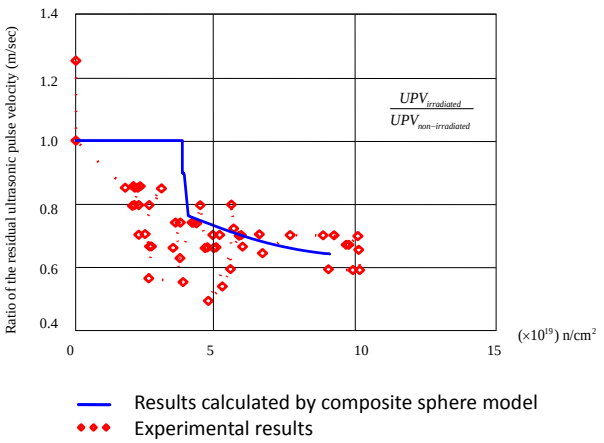

Figure 6: Comparison of ultrasonic pulse velocity between model predictions (blue line) and experimental results (red diamond symbol)

Figure 6 illustrates the comparison between experiments and simulations of the ratio of the ultrasonic velocity, defined as the ultrasonic velocity of an irradiated concrete over the same quantity of a sound concrete. We observe that the calculated ultrasonic pulse velocity remains constant in the first stage of irradiation then decreases once the critical energy is reached (slight decrease at the beginning then brutal decrease once the completely damaged zone appears). Compared to the experimental measurements marked by red diamond, the composite sphere model proved satisfactory in estimating the ultrasonic pulse velocity (resp. effective Young's modulus) of the concrete in the case where damage occurs in the matrix. However, it overestimates the ultrasonic pulse velocity (resp. effective Young's modulus) of the elastic concrete. The overestimation may be due to the fact that in our model damage develops only in the matrix while the aggregate behave elastically. The possible damage in the aggregate and the resulting reduction in its elasticity are not considered.

4 CONCLUSIONS

To accurately describe the mechanical behavior of a concrete subjected to aggregate expansion inducing microcracks, we have proposed an extended composite sphere model on the basis of [2]. We first describe the general features of the model and provide the analytical solutions to the concrete expansion. Then, to illustrate the predicting performance of the model, we compare its predictions with the available experimental measurements on two specific concretes and find a good accordance between them. However, in this first attempt of modeling, the damage in the aggregate due to the radiation exposure and the volumetric expansions of fine aggregates dispersed in the matrix are not considered. An extra research effort in this direction is required to improve the model predicting abilities. Moreover, introducing a time-dependent behavior for the matrix would allow a better description of the long-term material response.

REFERENCES

[1] I. Pignatelli, A. Kumar, R. Alizadeh, Y. Le Pape, M. Bauchy and G. Sant, "A dissolution-precipitation mechanism is at the origin of concrete ceep in moist environment." , *J. Chem. Phys.*, vol. 145, no. 5, American Institute of Physics (AIP), Aug. 2016.

[2] L. Dormieux and D. Kondo, “Exact solutions for an elastic damageable hollow sphere subjected to isotropic mechanical loadings,” *Int. J. Mech. Sci.*, vol. 90, pp. 25–32, Jan. 2015.
[3] D. Kondo, H. Welemane, and F. Cormery, “Basic concepts and models in continuum damage mechanics,” *Rev. Eur. Génie Civ.*, vol. 11, no. 7–8, pp. 927–943, Oct. 2007.
[4] P. Castañeda, “The effect of spatial distribution on the effective behavior of composite materials and cracked media,” *J. Mech. Phys. Solids*, vol. 43, no. 12, pp. 1919–1951, Dec. 1995.
[5] I. Maruyama *et al.*, “Development of Soundness Assessment Procedure for Concrete Members Affected by Neutron and Gamma-Ray Irradiation,” *J. Adv. Concr. Technol.*, vol. 15, no. 9, pp. 440–523, 2017.
[6] W. J. Weber, “Radiation-induced defects and amorphization in zircon,” *J. Mater. Res.*, vol. 5, no. 11, pp. 2687–2697, Nov. 1990.
[7] E. A. Eissa and A. Kazi, “Relation between static and dynamic Young’s moduli of rocks,” *Int. J. Rock Mech. Min. Sci. Geomech. Abstr.*, vol. 25, no. 6, pp. 479–482, Dec. 1988.
[8] J. J. Zhang and L. R. Bentley, “Factors determining Poisson’s ratio,” CREWES Research Report, vol. 17, p. 15, 2005.
[9] Instytut Nafty i Gazu – Państwowy Instytut Badawczy and M. Słota-Valim, “Static and dynamic elastic properties, the cause of the difference and conversion methods – case study,” *Nafta-Gaz*, vol. 71, no. 11, pp. 816–826, Nov. 2015.
[10] B. J. Lee, S.-H. Kee, T. Oh, and Y.-Y. Kim, “Evaluating the Dynamic Elastic Modulus of Concrete Using Shear-Wave Velocity Measurements,” *Adv. Mater. Sci. Eng.*, vol. 2017, pp. 1–13, 2017.
[11] E. Herve and A. Zaoui “n-layered inclusion-based micromechanical modelling.” . *Int. J. Eng. Sci.*, vol. 31, pp 1-10, 1993.
[12] L. F. Elleuch, F. Duboi, and J. Rappeneau, “Effects of neutron radiation on special concretes and their components.,” *Commis. Energ. At. Cent. Études Nucleaires Saclay Gif-Sur- Yvette Fr.*